



Corrosion resistance and friction of sintered NdFeB coated with Ti/TiN multilayers

Yuanyuan Cheng ^a, Xiaolu Pang ^{a,*}, Kewei Gao ^a, Huisheng Yang ^a, Alex A. Volinsky ^b

^a Department of Materials Physics and Chemistry, University of Science and Technology Beijing, Beijing 100083, China

^b Department of Mechanical Engineering, University of South Florida, Tampa, FL 33620, USA

ARTICLE INFO

Article history:

Received 2 July 2013

Received in revised form 7 October 2013

Accepted 22 October 2013

Available online 28 November 2013

Keywords:

Titanium nitride

Sputtering

Wear

Electrochemical impedance spectroscopy

Polarization

Fretting corrosion

ABSTRACT

Ti/TiN multilayers were deposited on sintered NdFeB by radio frequency magnetron sputtering. The film grain size decreased with the number of multilayers in the stack. Corrosion current density of sintered NdFeB with Ti/TiN multilayers was much lower than bare NdFeB. NdFeB with six periods of Ti/TiN multilayers exhibited good corrosion resistance in artificial saliva. Wear properties were characterized followed by the open circuit potential measurements. Friction and corrosion are interdependent. The Ti/TiN multilayers enhanced the corrosion resistance and decreased the wear volume. The joint action of corrosion and mechanical loading boosted the wear rate.

© 2013 Elsevier B.V. All rights reserved.

1. Introduction

NdFeB is a superior hard magnetic material. NdFeB permanent magnets have found applications in a wide range of fields due to NdFeB excellent magnetic properties, wide sources of raw materials and low price [1]. In recent years, NdFeB magnets have been used in a variety of engineering applications, including biomedical, automotive, acoustics, and consumer electronics [1,2]. At present, most widely used orthodontic magnetic material is the rare earth NdFeB. Since magnetic forces have advantages in traditional orthodontic applications [3,4], orthodontic magnetic materials have attracted researchers in the past twenty years [5,6]. However, poor corrosion resistance in various environments hinders further applications [7–11]. Active phases, such as Nd-rich and B-rich phases in NdFeB permanent magnets, facilitate easy corrosion in corrosion medium, which weakens magnetic properties, and turns NdFeB into powder-like, non-useable product. Thus, anti-corrosion surface treatment is very important for sintered NdFeB magnets [12]. NdFeB is an attractive material for dental implants [13], however, perennial reliability and stability, along with corrosion and wear resistance are of concern [14], thus a protective layer is required. In industry, electroplated Ni, Zn, and Ni/Cu/Ni coatings are generally applied because of their good corrosion performance and low processing cost. However, electroplating is often accompanied by environmental concerns and deterioration of magnetic properties [15].

In recent years, the Al/Al₂O₃ [16], Al/Cr, gas nitriding [17], along with TiN and Ti/TiN multilayer films have been also used to improve the surface performance. TiN is a hard physical vapor deposition (PVD) coating, widely used in wear and corrosion protection applications. Titanium nitride films have golden yellow color, high hardness and good chemical and metallurgical stability [18], good corrosion resistance and low coefficient of friction [19], can be deposited by PVD, and are biocompatible [20,21].

As an environmentally-friendly method, PVD has attracted increasing attention, and has been utilized to improve corrosion resistance [22–26]. PVD is a dry deposition technology, without liquid waste pollution, opposite to electroplating. It can also produce coatings with better adhesion to the substrate, which is critical for corrosion resistance in the oral cavity. Meanwhile, the efficiency of PVD has been enhanced in recent years [27]. This paper describes an experimental study of NdFeB corrosion protection with titanium nitride ceramic multilayer coatings in artificial saliva.

2. Experimental details

Sintered demagnetized NdFeB samples with composition given in Table 1, were ground to 20 mm × 20 mm × 3 mm dimensions and mechanically polishing to 5000 grit. The model of the NdFeB was N42H, provided by the SANVAC Company in China. Then the samples were cleaned for 15 min in acetone, followed by alcohol cleaning in an ultrasonic bath. Titanium nitride thin films were deposited on NdFeB by RF-magnetron sputtering at 300 °C. The vacuum chamber schematic is shown in Fig. 1. The base pressure was 5 × 10⁻³ Pa. First, the chamber

* Corresponding author.

E-mail address: pangxl@mater.ustb.edu.cn (X. Pang).

Table 1
NdFeB composition.

NdFeB (N42H)	B	Dy	Nd	Pr	Tb
wt.%	1.06 ± 0.06	0.7 ± 0.14	28.22 ± 0.60	0 ± 0.33	0.92 ± 0.03

was purged with high purity argon at 30 sccm (standard cubic centimeters per minute). Then, the specimens were cleaned by Ar⁺ ion bombardment with 50 W energy for 30 min. The coating deposition started at 300 W. To prepare Ti/TiN multilayers, alternating Ti and TiN films were deposited on sintered NdFeB, which was rotated to obtain homogeneous coatings. The Ti layers were deposited by RF magnetron sputtering from a 76 mm diameter titanium target. The TiN films were deposited by RF magnetron sputtering with Ar-N₂ mixed gas, in which the flow of N₂ was 1 sccm. Multilayers with different periods (Ti + TiN) were prepared with similar overall coating thickness. The deposition conditions are listed in Table 2.

The film thickness was measured with scanning electron microscopy (SEM) using ZEISS EVO18, and also with a Dektak 150 stylus profilometer. The titanium film deposition rate was about 11 nm/min. The deposition rate of the TiN film was 8.7 nm/min. The coating hardness was measured by nanoindentation. The structure of the Ti/TiN coatings was characterized using the field emission scanning electron microscope (FESEM, 10 kV). The friction coefficient of the NdFeB was measured before and after coating with the friction wear testing machine (UMT-2). Finally, the dynamic polarization curves were measured to explain the effect of Ti/TiN multilayers on NdFeB corrosion resistance with electrochemical workstation (CHI660C). The testing solution was artificial saliva with composition listed in Table 3. A conventional three-electrode cell was used with the Standard Calomel Electrode (SCE, saturated KCl) as the reference electrode and a platinum sheet (16 mm × 16 mm) as the auxiliary electrode. The exposed surface area of the working electrodes was 4 cm². To stabilize the stationary potential, all systems were kept in solutions for 1 h prior to measurements. Single round tests were performed at a scanning rate of 0.5 mV/s with the applied potential varied from −0.5 V (SCE) to 0.5 V (SCE), opposite to the open circuit potential. The range of the test frequency was 10^{−2}–10⁵ Hz, and the AC amplitude was 5 mV in the electrochemical impedance spectroscopy (EIS) test.

3. Results and discussion

3.1. Film morphology

Fig. 2 shows cross-sectional FESEM images of sintered NdFeB coated with Ti/TiN multilayers with one, three and six periods. The transition Ti layer is very thin, labeled in Fig. 2(a). TiN layer is 2.3 μm thick, with the

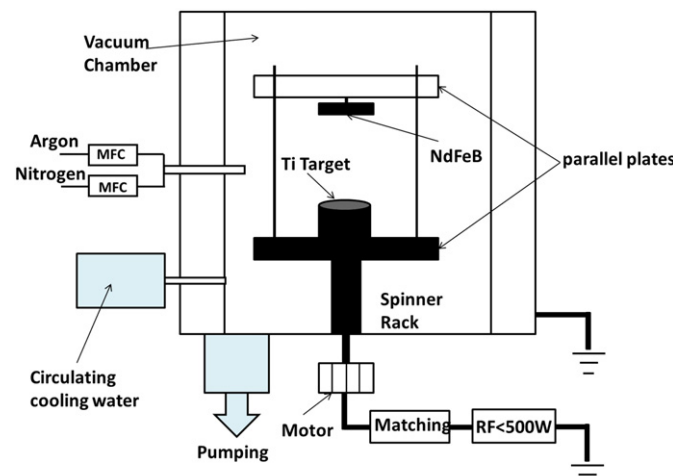


Fig. 1. Vacuum chamber schematic.

Table 2
Coatings deposition conditions.

Coating	Layer	Thickness of each layer	Coating overall thickness (μm)	Gas flow rate	
				Ar (sccm)	N ₂ (sccm)
Single layer	Ti	200 nm	2.5	30	–
	TiN	2.3 μm		30	1.0
3 periods of Ti/TiN multilayers	Ti	150 nm	2.35	30	–
	TiN	Others 600 nm		30	1.0
6 periods of Ti/TiN multilayers	The top 1 μm				
	Ti	90 nm	2.54	30	–
	TiN	Others 200 nm		30	1.0
The top 1 μm					

columnar grain structure. In Fig. 2(b), the TiN layer also has columnar structure. The top layer has bulky crystal structure, and the Ti/TiN coatings have obvious stratification. Ti/TiN multilayers with six periods also have Ti layer and columnar TiN layer, seen in Fig. 2(c). However, the structure with six periods is denser than with one or three periods. The film becomes denser with the number of layers, and the number of defects is reduced. Ti layer breaks down columnar structure of the TiN coating, and as a result, the grain boundaries between columnar grains in different Ti layers are independent. Therefore, penetrating micropores, which act as fast diffusion paths for aggressive media, could be inhibited in multilayers. Furthermore, the micropores would be further inhibited with more periods in the multilayer as a result of the increased interfacial area. In addition, the alternating structure suppresses penetration of the test solution, and therefore, the long-term electrochemical stability of the coated samples is improved. The multilayer structure can redistribute the current flow to eliminate current concentration at the small pinholes and prevent rapid galvanic attack at the pits [28]. Moreover, the compact structure allows the corrosion products to plug the micro-corrosion holes more efficiently. Thus, Ti/TiN multilayers can have better anticorrosion performance. Typical X-ray diffraction (XRD) θ/2θ scans from reactively magnetron-sputtered multilayers Ti/TiN coatings deposited with different layers on bare sintered NdFeB substrates are presented in Fig. 3.

3.2. Corrosion-resistant properties

The anti-corrosion performance of the uncoated NdFeB magnet and the magnets with Ti/TiN multilayer films in the artificial saliva was studied, and compared using open circuit potential, EIS and potentiodynamic polarization techniques. From Fig. 4, it can be seen that the open circuit potential of the bare sintered NdFeB (1) is clearly lower than the NdFeB with Ti/TiN multilayers. Meanwhile, the open circuit potential increases with the number of film layers.

Fig. 5 displays the EIS spectra tested in artificial saliva. The magnets with Ti/TiN coatings have the best corrosion resistance. The bare sintered NdFeB (Fig. 5a) has an added Warburg circuit element for the uncoated magnet, which indicates the occurrence of the preferential corrosion along particle boundaries [29,30]. The EIS spectra also show that the Ti/TiN multilayer films clearly improve the anticorrosion performance of NdFeB magnets. Fig. 5b shows the radius of curvature with the three kinds of coating films, which is larger than the bare sintered NdFeB. The equivalent circuit is obtained by the Zview 2 software, as shown in Fig. 5. The low frequency capacitive loop is quite complicated. From the equivalent circuit one can get the polarization resistance (R_p), along with the double layer capacitance (the constant phase element, CPE, is used to account for the non-ideal capacitive

Table 3
Artificial saliva composition.

Salivary components	KCl	NaCl	CaCl ₂ ·2H ₂ O	Na ₂ S·9H ₂ O	NaH ₂ PO ₄ ·2H ₂ O	Urea
g/L	0.400	0.400	0.906	0.005	0.696	1.000

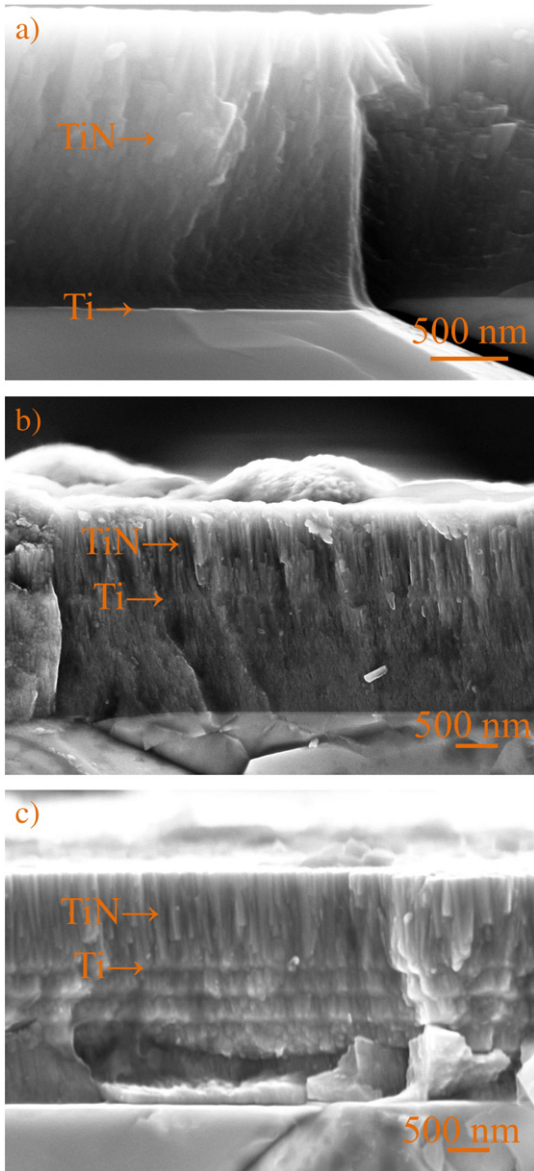


Fig. 2. Field emission cross-sectional images of sintered NdFeB coated with: (a) single, (b) three and (c) six periods of Ti/TiN multilayers.

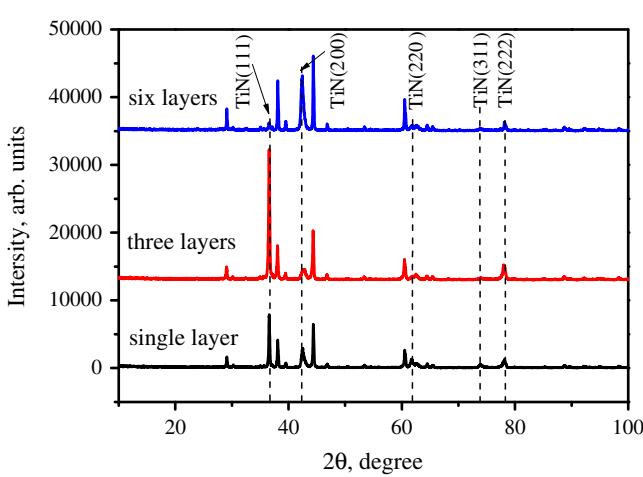


Fig. 3. XRD spectra of different layers of Ti/TiN multilayers on bare sintered NdFeB.

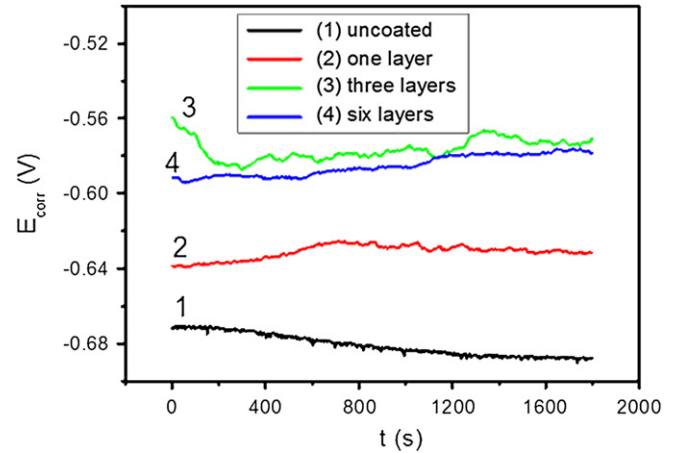


Fig. 4. Open circuit potential curves of (1) bare sintered NdFeB, and coated with (2) single, (3) three, and (4) six periods of Ti/TiN multilayers in artificial saliva.

response, instead of capacitance). The equivalent circuit model is shown in Fig. 6. The impedance of CPE is given as:

$$Z_{CPE} = 1/[Y_0(j\omega)^\eta] \quad (1)$$

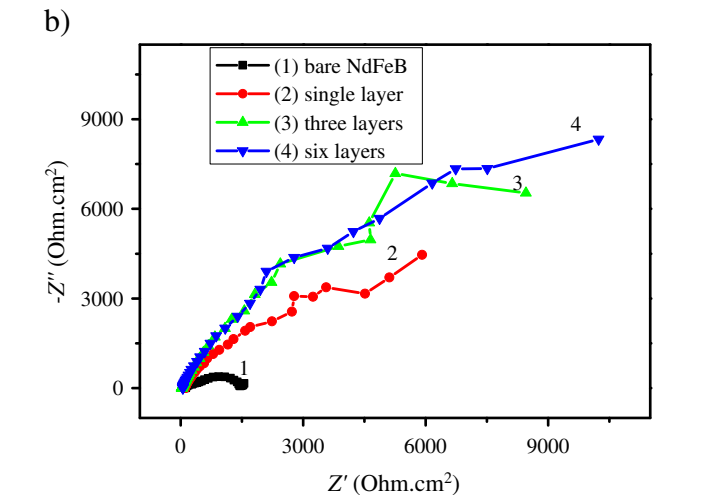
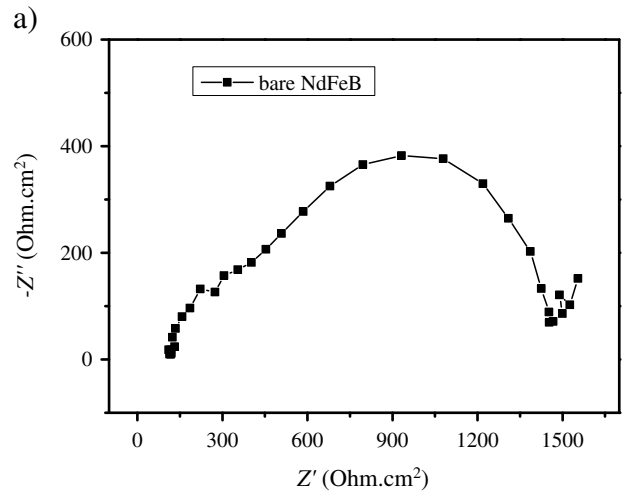


Fig. 5. EIS spectra of (a) bare sintered NdFeB, (b) uncoated NdFeB (1) and coated with (2) single, (3) three and (4) six periods of Ti/TiN multilayers in artificial saliva.

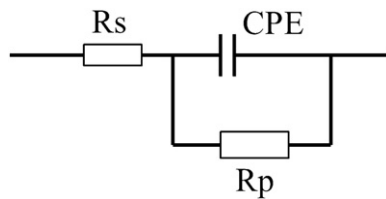


Fig. 6. Equivalent circuit model for the samples immersed in artificial saliva.

Table 4
Analyzed values of the equivalent circuit parameters.

Sample	R_p ($\text{K}\Omega \cdot \text{cm}^2$)	Y_0 ($\Omega^{-1} \cdot \text{cm}^{-2} \cdot \text{s}^{-1}$)	η ($0 < \eta < 1$)
Bare sintered NdFeB	6.10	8.8×10^{-4}	0.74
Single layer	9.52	5.8×10^{-4}	0.75
Three layers	22.80	5.1×10^{-4}	0.76
Six layers	19.00	4.0×10^{-4}	0.89

where Y_0 is the admittance magnitude of the CPE and η is the power index number. It is well known that the CPE is affected by the properties of the coating, such as surface roughness, porosity, and so on [31,32]. This paper explains the difference of R_p in the uncoated and coated NdFeB magnets. In Table 4, the values of R_p increase from the top to the bottom, and the three and six periods of Ti/TiN multilayers have the maximum values. Besides, the values of Y_0 decreased in the uncoated and coated NdFeB magnets, because rust began to block the pinholes [32], leading to some loss in the corrosion protection. This suggests that magnets with Ti/TiN composite films have the best anticorrosion properties.

Fig. 7 shows potentiodynamic polarization curves of bare sintered NdFeB, and with the single layer, three and six periods of Ti/TiN multilayers. Measured anode curves were different from the cathode curves. The four lines of the cathode curves almost overlapped. However, the current density of the bare sintered NdFeB changed quickly with the potential increasing in the anode curves. Sample coated with Ti/TiN multilayers with six periods showed better corrosion resistance, as the current density changed slowly with the voltage increase. The corrosion potential, E_{corr} , and corrosion current density, i_{corr} , values, calculated by the CVView2 software are listed in Table 5. The corrosion potential of the uncoated NdFeB specimen was approximately -0.7 V (vs. SCE), whereas those of the NdFeB specimen with one, three, and six periods of Ti/TiN multilayers were about -0.44 V (vs. SCE), -0.49 V (vs. SCE), and -0.55 V (vs. SCE). The most important thing turned out to be the comparison of the current density. The corrosion current density of the bare sintered NdFeB specimen was about 2829 nA/cm 2 . For the NdFeB

Table 5

Polarization data obtained from the bare sintered NdFeB and coated with a single layer, three and six periods of Ti/TiN multilayers in artificial saliva.

Samples	E_{corr} (V)	i_{corr} (nA/cm 2)
Bare sintered NdFeB	-0.70	2829
Single layer Ti/TiN	-0.44	523
Three periods of Ti/TiN multilayers	-0.49	98
Six periods of Ti/TiN multilayers	-0.55	28

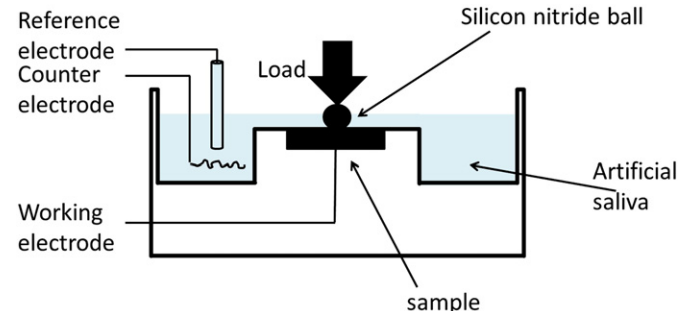


Fig. 8. Schematics of the UMT-2 friction testing machine.

specimens coated with the single layer, i_{corr} was approximately 523 nA/cm 2 . It was found that the single layer Ti/TiN coating clearly protects NdFeB. The corrosion current density of the sintered NdFeB coated with Ti/TiN multilayers is much lower than that of the bare sintered NdFeB. This demonstrates that corrosion resistance of the sintered NdFeB was effectively improved by these coatings. Also, the current density of the Ti/TiN multilayers with six periods was only 28 nA/cm 2 , about two orders of magnitude lower than that of the bare sintered NdFeB specimen. This indicates that the corrosion resistance of the sintered NdFeB became much better, and improved with the number of multilayers. The corrosion rate and the current density followed the same trend.

3.3. Friction and wear

Fig. 8 shows schematics of the friction wear testing machine (UMT-2). Bare sintered NdFeB and NdFeB coated with a single layer and six periods of Ti/TiN multilayers were tested. The following test parameters were used: 5 mm diameter Si₃N₄ ball, 5 N normal load, 15 mm scratch length, and 1 h total testing time. The sample was left for 10 min before and after each friction test. Fig. 9 shows the friction coefficient of bare

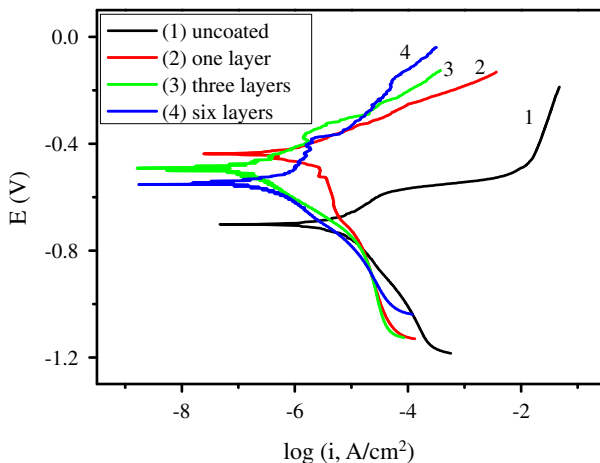


Fig. 7. Potentiodynamic polarization curves of (1) bare sintered NdFeB, and coated with (2) single, (3) three, and (4) six periods of Ti/TiN multilayers in artificial saliva.

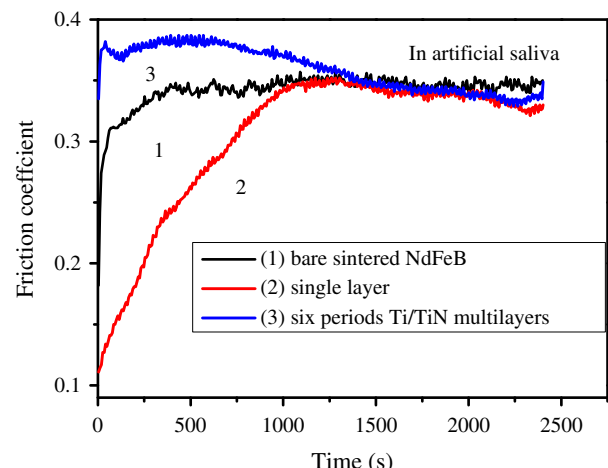


Fig. 9. Friction coefficient of (1) bare sintered NdFeB and coated with (2) a single layer and (3) six periods of Ti/TiN multilayers in artificial saliva.

sintered NdFeB and NdFeB coated with the single layer and the six periods of Ti/TiN multilayers in solution. The friction coefficient of the three tested samples is almost the same at the steady state. However, the friction coefficient of the three tested samples exhibits a large difference at the initiation of the test. The reasons for this phenomenon are due to the running-in stage [33] and the friction coefficient being related to many potential factors, like surface conditions, the macromechanical properties of the contact surface and so on [34]. This stage is quite complicated, thus that the friction coefficient is not stable at the initiation of the test. The main result though is that titanium nitride coatings didn't change the friction coefficient of the bare NdFeB. However, a large difference in the wear tracks is seen in Fig. 10, which were obtained in artificial saliva in Fig. 10(a, b, c), and in air in Fig. 10(d, e). The wear track width shows that the bare sintered NdFeB didn't wear more than with the Ti/TiN multilayers, however, corrosion of bare NdFeB was more severe in Fig. 10a. The wear track is smoother with Ti/TiN multilayers in the simulated environment

Table 6

Wear capacity of bare NdFeB, with a single Ti/TiN layer and with six periods of Ti/TiN multilayers in different environments.

Samples	Wear volume in solution ($\times 10^{-3} \text{ mm}^3$)	Wear volume in air ($\times 10^{-3} \text{ mm}^3$)
Bare sintered NdFeB	1.1356	0.6897
Single layer	0.5794	2.0247
Six periods of Ti/TiN multilayers	0.1789	4.6164

(Fig. 10b, c) than in air (Fig. 10d, e). The wear volume was measured using a Dektak 150 stylus profilometer, listed in Table 6. The wear volume of bare NdFeB magnets was $1.136 \times 10^{-3} \text{ mm}^3$ larger than with the Ti/TiN multilayers in the solution. Furthermore, the wear volume gradually reduced with the number of Ti/TiN periods in

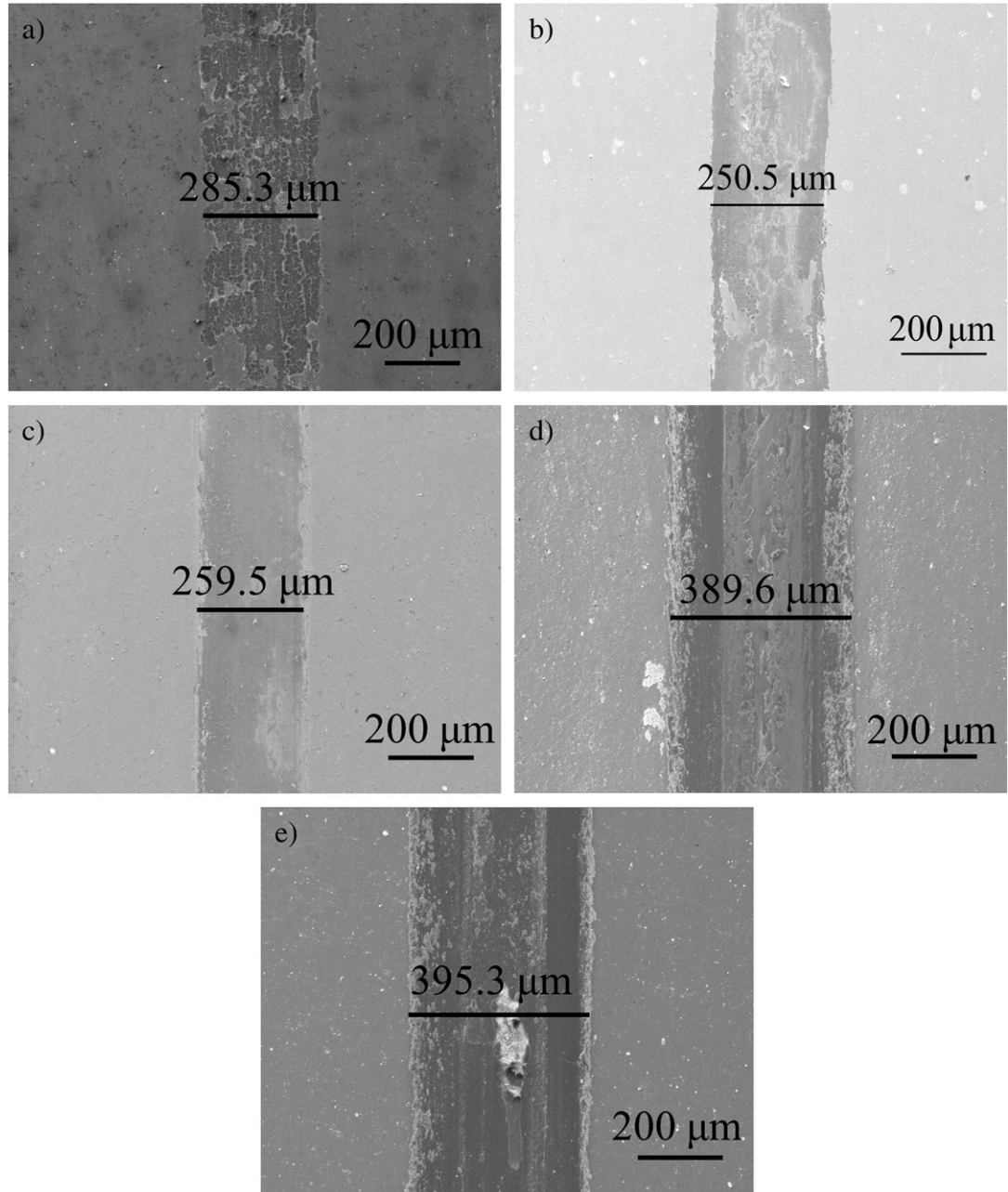


Fig. 10. SEM images of the wear tracks on (a) bare sintered NdFeB, (b) single layer and (c) six periods of Ti/TiN multilayers in artificial saliva; (d) single layer and (e) six layers in air.

Table 7

EDS composition analysis of the wear track in dry friction measurements.

Sample/at.%	C	N	O	Si	Ti
The single layer	7.3	11.5	55.3	1.7	24.2
The six layers	15.1	0.4	50.4	4.1	14.5

the multilayer stack. However, an opposite result was observed in air. Obviously, the wear volume increased with the Ti/TiN multilayers. The main difference between the solution and air is that there is corrosion in the solution. Meanwhile, the wear track of the multilayers Ti/TiN coating in Fig. 10(d, e) shows many cracks with silicon and oxygen found by the energy dispersive spectroscopy (EDS) at 20 kV under high pressure, listed in Table 7. These results indicate that adhesion and the oxidation reactions happen during the friction measurements in dry conditions. Besides, the peeling abrasive dust also plays an important role in friction measurements. However, adhesion was not observed during wear testing in the wet environment. As a result, adhesion wear is a predominant mechanism, and almost no abrasive was present during dry testing. However, only abrasive wear was observed in the simulated saliva environment. The interaction between corrosion and wear usually degrades performance. However, some tests found that the material loss is smaller in corrosion medium than during dry friction in air [35]. Such phenomenon was observed with the Ti/TiN multilayers, thus there could be negative interaction in these tests. Combined action of corrosion and mechanical loading can accelerate the corrosion wear rate. Thus, based on our results, the main reasons why the multilayered Ti/TiN coating offers better corrosion wear resistance in artificial saliva environment are: (1) the multilayer Ti/TiN coating has anticorrosion properties; (2) the solution acts as a lubricant and reduces friction.

Fig. 11 shows the corrosion potential, E_{corr} , values for different samples in the artificial saliva. The open circuit potential of the bare NdFeB magnets was much lower. An obvious change was observed as soon as the load was added at 600 s, and the values stabilized over time. These results explain lower wear volume of the Ti/TiN coated samples, which improved corrosion resistance in the friction wear test.

3.4. Coating hardness

Hardness, H , is an important thin film mechanical property that can be measured using nanoindentation techniques. In this experiment, the nanoindentation loading rate was 10 nm/s and the values of hardness and elastic modulus were the average values from loading displacement between 1/7 and 1/10 of the Ti/TiN film thickness. The results shown in Fig. 12, depend on the film microstructure. Coated samples are obviously harder than the bare sintered NdFeB. The hardness of the bare sintered NdFeB is around 9 GPa. However, the hardness of NdFeB

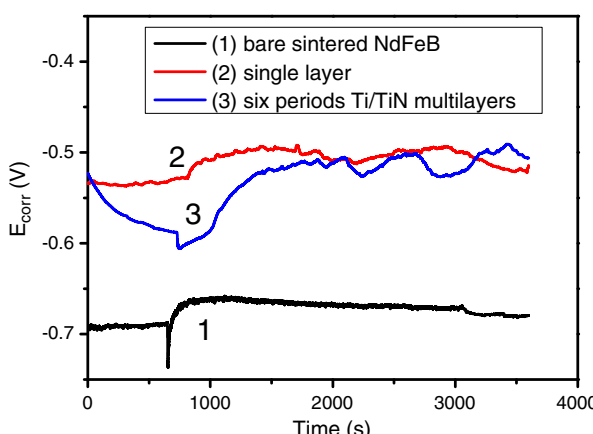


Fig. 11. E_{corr} time dependence of the bare sintered NdFeB, the single layer and the six periods of Ti/TiN multilayers tested for 1 h in artificial saliva.

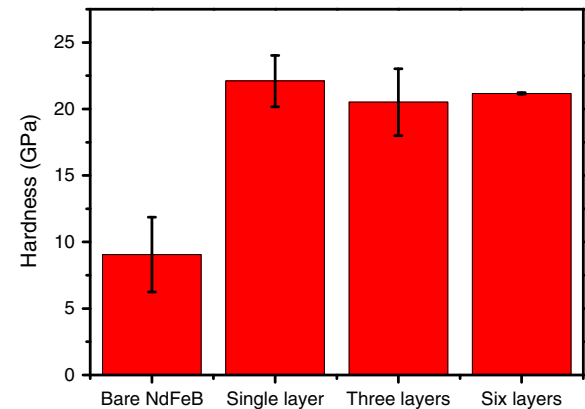


Fig. 12. Hardness of bare sintered NdFeB and coated with a single layer, three and six periods of Ti/TiN multilayers measured by nanoindentation.

magnets coated with the single layer, three and six periods of Ti/TiN multilayers is about 2.5 times higher than the bare NdFeB sample. Hardness only changed slightly with the number of periods in the Ti/TiN multilayer stack. Bare sintered NdFeB hardness is significantly improved by the Ti/TiN multilayer coatings, along with friction, wear and corrosion resistance.

4. Conclusions

Ti/TiN coatings were deposited on bare sintered NdFeB by radio frequency magnetron sputtering and significantly improved bare sintered NdFeB corrosion resistance. The Ti/TiN coating included Ti layer and crystalline columnar TiN film. As the number of the periods increased, TiN columnar grains were terminated by the Ti layer and limited TiN columnar growth in the multilayer stack. These coatings improve bare NdFeB corrosion resistance. Thus, the current density of the coated samples diminished, and the polarization resistance increased, showing better corrosion resistance. Ti/TiN multilayers with six periods showed the best performance in terms of corrosion protection. The friction wear test performed in artificial saliva also showed that the Ti/TiN multilayers improved corrosion resistance. The wear volume of bare sintered NdFeB surface in solution was the largest. The wear volume in different environments was compared. Ti/TiN multilayers deposited on bare NdFeB improved friction and wear resistance. The material loss is smaller in corrosion medium than in air, proving that corrosion limited mechanical wear. The interaction between corrosion and wear has a negative effect. The hardness of the Ti/TiN multilayer coating was 2.5 times higher than the bare sintered NdFeB.

Acknowledgments

This work was supported by the National Nature Science Foundation of China (51001013, 51271022), the Fok Ying Tung Education Foundation (132001) and the Fundamental Research Funds for the Central Universities.

References

- [1] M. Sagawa, S. Fujimura, N. Togawa, H. Yamamoto, Y. Matsuura, J. Appl. Phys. 55 (1984) 2083.
- [2] J.J. Croat, J.F. Herbst, R.W. Lee, F.E. Pinkerton, J. Appl. Phys. 55 (1984) 2078.
- [3] M. Muller, Eur. J. Orthod. 6 (1984) 247.
- [4] M.A. Darendeliler, M. Chiariini, J.P. Joho, J. Clin. Orthod. 27 (1993) 563.
- [5] T. Kawata, S. Takeda, J. Dent. Res. 56A (1977) 189.
- [6] T. Kawata, K. Hirota, K. Sumitani, Am. J. Orthod. 92 (1987) 241.
- [7] J. Jacobson, A. Kim, J. Appl. Phys. 61 (1987) 3763.
- [8] L. Schultz, A.M. El-Aziz, G. Barkleit, K. Mummert, Mater. Sci. Eng. A 267 (1999) 307.
- [9] I. Gurappa, J. Alloys Compd. 360 (2003) 236.
- [10] A.A. El-Moneim, A. Gebert, J. Appl. Electrochem. 33 (2003) 795.
- [11] A.A. El-Moneim, Corros. Sci. 46 (2004) 2517.
- [12] C.J. Willman, K.S.V.L. Narasimhan, J. Appl. Phys. 61 (1987) 3766.

- [13] H. Akin, M.E. Coskun, E.G. Akin, A.K. Ozdemir, J. Prosthet. Dent. 105 (2011) 203.
- [14] H. Akin, A.K. Ozdemir, J. Dental Sci. 8 (2012) 184.
- [15] H. Yang, S. Mao, Z. Song, Mater. Corros. 62 (2011) 1.
- [16] S.D. Mao, H.X. Yang, F. Huang, T.T. Xie, Z.L. Song, Appl. Surf. Sci. 257 (2011) 3980.
- [17] D. Starosvetsky, I. Gotman, Biomaterials 22 (2001) 1853.
- [18] F.J. Espinoza-Beltrán, O. Che-Soberanis, L. García-González, J. Morales-Hernández, Thin Solid Films 437 (2003) 170.
- [19] C.T. Kao, S.J. Ding, Y.C. Chen, J. Biomed. Mater. Res. 63 (2002) 786.
- [20] A. Steinert, C. Hendrich, F. Merklein, P.C. Rader, N. Schütze, R. Thull, J. Eulert, Biomed. Technol. 45 (2000) 349.
- [21] K. Bordji, J.Y. Jouzeau, D. Mainard, E. Payan, P. Netter, K.T. Rie, T. Stucky, M. Hage-Ali, Biomaterials 17 (1996) 929.
- [22] C.H. Lin, J.G. Duh, Surf. Coat. Technol. 203 (2008) 558.
- [23] E.M. Pinto, A.S. Ramos, M.T. Vieira, C.M.A. Brett, Corros. Sci. 52 (2010) 3891.
- [24] M. Flores, L. Huerta, R. Escamilla, E. Andrade, S. Muhl, Appl. Surf. Sci. 253 (2007) 7192.
- [25] Y.H. Yoo, J.H. Hong, J.G. Kim, H.Y. Lee, J.G. Han, Surf. Coat. Technol. 201 (2007) 9518.
- [26] M. Reffass, C. Berziou, C. Rebere, A. Billard, J. Creus, Corros. Sci. 52 (2010) 3615.
- [27] B. Navinsek, P. Panjan, I. Milosev, Surf. Coat. Technol. 116–119 (1999) 476.
- [28] R.S. Liliard, D.P. Butt, T.N. Taylor, K.C. Walter, M. Nastasi, Corros. Sci. 39 (1997) 1605.
- [29] C.B. Ma, F.H. Cao, Z. Zhang, J.Q. Zhang, Appl. Surf. Sci. 253 (2006) 2251.
- [30] Cheong Woo-Jae, Ben L. Luan, David W. Shoesmith, Corros. Sci. 49 (2007) 1777.
- [31] J. Creus, H. Mazille, H. Idrissi, Surf. Coat. Technol. 130 (2000) 224.
- [32] S.H. Ahn, J.H. Lee, J.G. Kim, Surf. Coat. Technol. 177–178 (2004) 638.
- [33] Y. Yan, A. Neville, D. Dowson, Appl. Phys. 39 (2006) 3200.
- [34] P.J. Blau, Tribol. Int. 34 (2001) 585.
- [35] X.X. Jiang, S.Z. Li, C.T. Duan, M. Li, Wear 129 (1989) 293.